ARMA/USRMS 06-1118

Dynamic fragmentation of rock by high-voltage pulses

S.H. Cho and B. Mohanty

Lassonde Institute and Department of Civil Engineering, University of Toronto, Toronto, Canada

M. Ito

Graduate School of Engineering, Hokkaido University, Sapporo, Japan

Y. Nakamiya and S. Owada

Department of Resources and Environmental Engineering, Waseda University, Tokyo, Japan

S. Kubota, Y. Ogata,

National Institute of Advanced Industrial Science and Technology (AIST), Japan

A. Tsubayama

Department of Materials process Engineering, Akita University, Akita, Japan

M. Yokota and K. Kaneko

Faculty of Engineering, Hokkaido University, Sapporo, Japan

ABSTRACT: The purpose of this study is to develop a high-precision disintegration technology for extracting industrial minerals from rock matrices by applying high-voltage electrical pulses. The electrical disintegration of rock through application of high voltage electrical pulse is one of the effective liberation techniques for producing the high percentage of the monomineral particles in disintegration of mineral aggregates. Circular rock samples of three different types were fractured by electric pulses. The microstructure and fractures of the test samples were visualized and analyzed by using microfocus X-ray computed tomography (CT) system. The fracture patterns are simulated by using the dynamic fracture process analysis code and the fragmentation process resulting from electrical pulses are discussed. The influence of rock heterogeneity and sample size effect on the dynamic fragmentation is also discussed.

1. INTRODUCTION

The availability of an efficient breakage method for separating constituents of a rock is of interest to researchers or engineers interested in highly effective comminution for recovering useful minerals, single crystal separation for crystal structure determinations and individual microfossil separation. There has been an issue of interest for the last several decades in the use of high-voltage pulse technology for rocks disintegration. The methods of electric pulse disintegration are mainly electrohydraulics and internal breakdown inside bulk solid dielectrics [1-7]. The first method refers to the generation of an intense shock wave in water from the passage of electrical current through water and the crushing and subsequent constituent separation by the impact of that shock wave on the sample. The second method refers to the passage of electrical current through the rock and the separation of the mineral contents from the rock matrix by preferential current flow along the mineral/rock boundary interface. Rock disintegration using the second method consumes substantially less energy than that using the first method and enhanced effect of liberation of mineral constituents of rock aggregates [1,3]. Almost studies have described the sequence of dielectric events and resultant fractures but do not include a fracture process of rock by high-voltage pulses.

The pulsed power technology has been also applied to rock excavation, liberation of micro-fossils, drilling of rocks, oil and water stimulation, casting cleaning, and recycling of products such as concrete, electronic devices and electric appliances [7-9]. In order to obtain a higher yield of precious constituents, while conserving their original size and shape, the separations or breakages must mainly occur at the boundaries of the constituents. A recent study indicated that tensile cracks and branching cracks caused by the reflected waves from the free surfaces are important to separate the constituents and the number increasing of radial cracks generated from the electric pulse channel decreases the productivity of mineral particles [10].

In this study, 5 mm thick circular rock samples of three different types were fractured by high-voltage pulses. The discharge voltage and current were measured and the fracture process in the test was photographed by a high speed camera (Shimadzu, HPV-1), with a recording speed of 1 Mfps. The microstructure and fractures of the rock samples were visualized and analyzed by using microfocus X-ray computed tomography (CT) system before and after the tests. The fracture patterns are simulated by using the dynamic fracture process analysis code [11] and the fragmentation process resulting from electrical pulses discussed. The electric pulse dynamics and dynamic fracture process of rock are studied in detail. This study will allow the optimization of the discharge parameters form the viewpoint of the dynamic fragmentation in a solid dielectric, improving the fracture controlling efficiency.

2. EXPERIMENTS

2.1 Experimental set-up

To initiate the electric discharge, the arrangement schematically drawn in Figure 1 is used. The experiment apparatus is installed in the Akita University, Japan. The current flow was measured by the current transformer, and the current and voltage waveforms were monitored by the digital oscilloscope. The high speed camera, with a recording speed of 1 Mfps, was used to observe the electric pulse breakdown of rock samples.

The rock samples were placed between two electrodes and immersed in water to decrease the corona discharge. The high voltage electrode

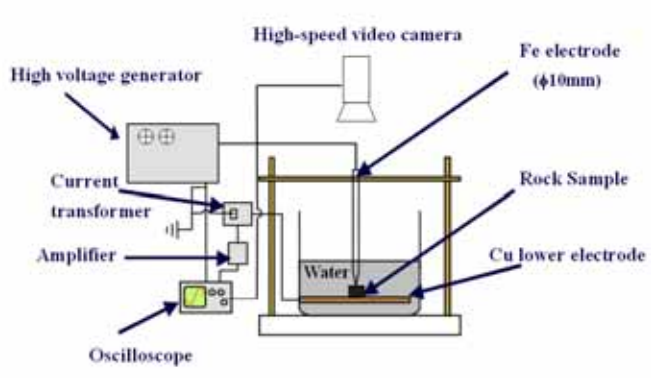

Fig. 1 Schematic diagram of high-voltage pulse breakage test

(ϕ10mm) and the grounded electrode (plate) are made of iron and copper, respectively.

Table 1 lists the properties of Inada granite, Shikotsuko welded tuff, and Shirahama sandstone samples, and test conditions. The preliminary tests were conducted to investigate the value of charging voltage, which is able to fracture the samples. The voltages of granite rock samples were closed to the maximum capacitance of the pulse generator. The round of the samples was applied by silicone gum to avoid the flying of fragments. Inada granite consists of quartz (34% by volume), alkali-feldspar (24%), plagioclase (33%), biotite and other minerals (6%). The mean grain size is about 2.0 mm [13]. Shikotsuko welded tuff consists of minerals (25%), matrix (40%) and porous (35%). Shirahama sandstone consists of quartz (22.5% by mode analysis), plagioclase (29.9%), muscovite (0.1%), rock fragment (8.3%), calcite (2.5%) and matrix (36.7%). The grain size ranges from 125~250μm.

Table 1 Properties of the samples applied voltages

Materials	Density (g/cm^3)	Elastic Wave velocity (km/s)	Diameter (thickness) ,cm	Tensile strength (MPa)	Set voltage (kV)
Inada Granite	2.60	3.63	2, 3, 5(0.5)	6.9	74-88
Shikotuko Tuff	2.23	3.21	3 (0.5)	3.2	40-70
Shirahama Sandstone	1.39	2.45	3 (0.5)	3.3	40-70

2.2 Measurement of voltage and currents

We used the system shown in Fig. 1 to load a high-voltage pulse on the rock samples. The voltage of the positive polarity was applied to upper electrode, which is placed in the middle of the samples, and the other electrode was grounded. The applied voltage and discharged current were measured for all tests.

Figure 2 shows a typical voltage and current waveform. The waveforms can be characterized into phases I, II and III. In the phase I, the voltage increased suddenly and reached the peak value within 0.1 μs without increasing current. Then the voltage rapidly dropped with increasing of the current in phase II. The current reached with the rising time of 0.6 μs in phase III. Consider previous researches[1-9], it is conceivable that in the phase III the mechanical stresses caused by the high current flowing along the arc plasma channel, which is completed in the solid dielectric during phase II, results in the rock fragmentation.

Table 2 summarizes the results of the measured waveforms. The discharged currents tend to increase with increasing applied voltages on regardless of the rock type as plotted in Figure 3. The current rise times for the granite samples were shorter than the other rock samples. The tuff samples showed the longer rise times. It is possible that higher rise time of current increases the mechanical stress loading rate.

Figures 4 (a)-(e) show the examples of the fractured samples by high-voltage pulses.

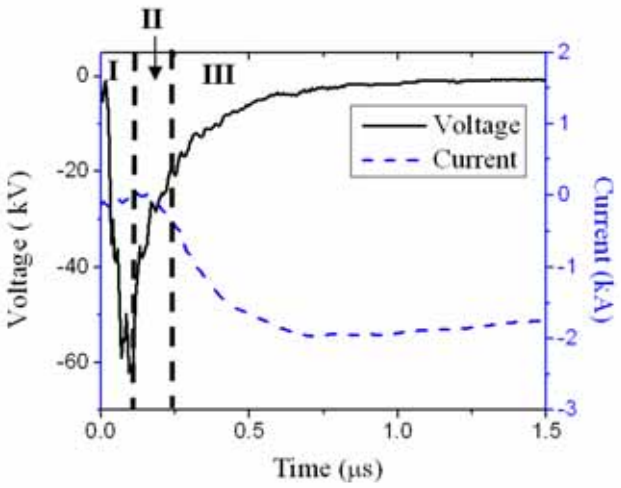

Fig. 2 Measured waveforms of voltage (solid) and current (dashed) for a granite sample.

Table 2 Summary of high-voltage pulse fracture tests

Materials	Applied Voltage (kV)	Discharged Current (kA)	Current rise time t_c(μs)	No. of Fragments	No. of Fragments (CT scans)
Granite	53.6	1.812	0.8	8	13
(D:ϕ2cm)	62.0	1.78	0.60	7	14
Granite	62.0	1.999	0.675	6	6
(D: ϕ3cm)	62.0	2.03	0.6	7	9
	60.8	1.99	0.44	6	8
	62.0	1.99	0.48	6	10
Granite	62.0	2.06	0.7	3	
(D: ϕ5cm)	62.0	1.62	0.63	4	
Tuff	36.6	0.969	0.92	2	3
	50.6	1.09	1.01	3	3
	46.4	1.469	1.01	4	5
	51.8	1.81	1.01	4	4
Sandstone	40.8	0.68	0.92	3	4
	41.8	1	0.8	4	4
	47.0	1.25	0.83	5	6
	52.8	1.37	0.83	5	5

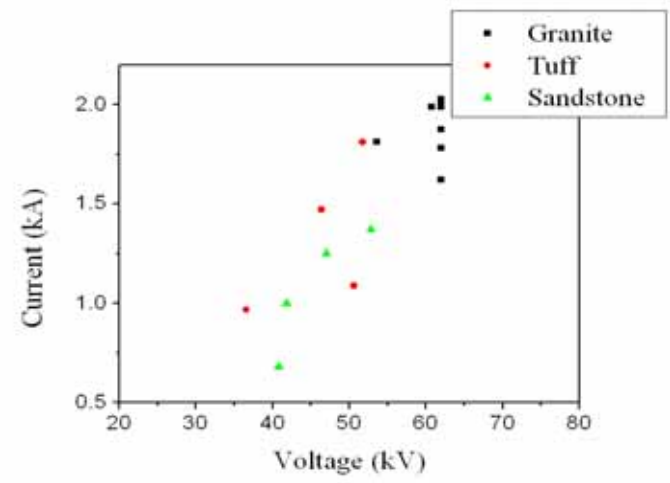

Fig. 3 Measured voltages vs. currents for all test samples

The radial tensile fractures develop around the crushed zone, which occur along the discharged path. The number of fragments in the granite rock samples decreases with the diameter increase as listed in Table 2. This could be caused by the effect of reflected waves from the surface on the crack formation. The number of fragments for the granite samples with 3 cm diameter ranges from 6 to 7, while tuff and sandstone samples show 3-5 fragments. This implies that the induced stresses in the granite samples, which show shorter current rise

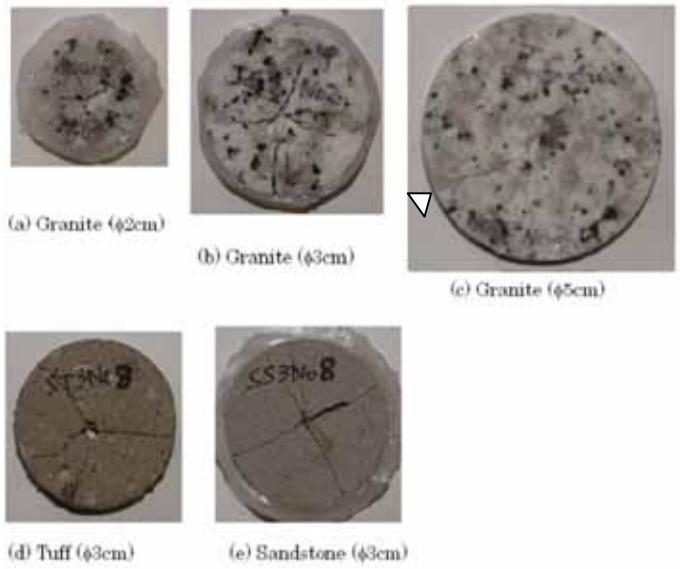

Fig. 4 Resultant fracture patterns of the tested rock samples

time, are greater than that in tuff and sandstone samples.

2.3 Fragmentation process of rock by high-voltage pulses

The optical images of the high voltage discharge were taken by high-speed video camera to observe the rock breakage by high-voltage pulses. The framing images taken during the early stages of the discharge show the appearance of one or more light emitting in the vicinity of the upper electrode. In the most of shots, the flashover retained for several tens micro-second and obstructed the observation of fracturing. The intensity of the flashover was also varied for every test. Expansion of bubble from the tip of the upper electrode was also observed for the all tests.

Figure 5 shows images photographed by the high-speed camera. The crack, which is indicated by the triangle in Fig. 4(c), is visible at 104 μs. This implies the crack formation in the samples is already completed within 100μs. The arrows indicate the outer boundary of the bubble and the expansion velocity of the bubble was 15 m/s. In order to investigate the behavior of the bubble, rough framing rate was examined. It was realized that the bubble disappears after 3ms and then fragments disperse.

Figure 6 illustrate the fragmentation process of rock by high-voltage pulse considering the measurement of voltage and current and high-speed camera

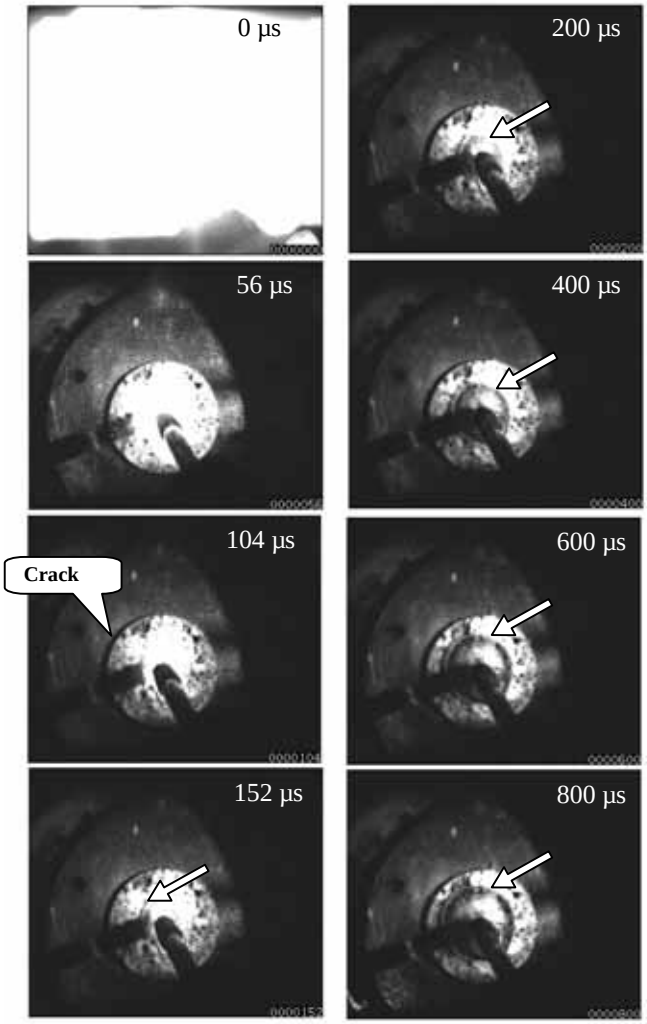

Fig. 5 Images photographed by high-speed camera for granite sample test; Frame rate: 8 μs/frame

observation. The fragmentation process can be explained as follows.

1) In phase I, formation of the breakdown channel into the rock from the applied electrode with light emitting and propagation of the voltage discharge inside the rock; here the voltage increases suddenly and reaches the peak value within 0.1 μs without increasing current.
2) In phase II, formation of the current flow channel (or arc plasma channel) between two electrodes; the voltage rapidly drops with increasing of the current.
3) In phase III, generation of mechanical stress caused by the expanding current flow channel; the current reaches the peak value within 1μs.
4) Crack propagation (mainly radial cracks) and crushing caused by the induced stress during several tens micro-second; while a bubble expands speedily over ten m/s.

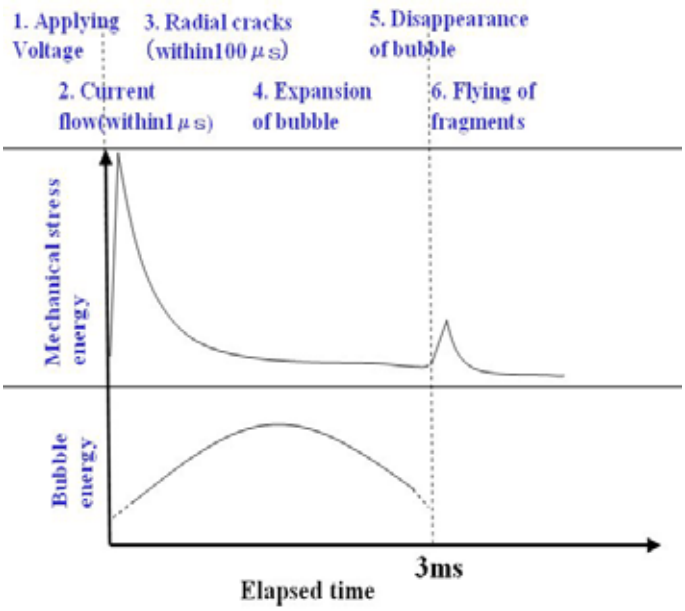

Fig. 6 Conceptual explanation of rock fragmentation by high-voltage pulses

5) Finally, disappearance of bubble after 3 ms and dispersion of fragments.

3. MICROSCOPIC ANALYSIS OF TESTED SAMPLES BY MICRO-FOCUS X-RAY CT

High-resolution X-ray CT has been used to observe microstructure of mineral particles and rock samples. In this study, we used the custom designed micro X-ray CT system (TOSCANER 30900μhd), which is installed at Hokkaido University [13], to observe the high-voltage induced-fractures inside the test samples. All tested rock samples were scanned covering theirs diameter and 5 mm high except for the granite samples with 50 mm diameter.

Figures 8 (a)-(c) show the cross sectional images of the rock samples, which have 30 mm diameter. The dotted circle indicates the estimated current flow path. In Fig. 8 (a), granite constituents and cracks are visible. The contrast in the images shows differences in the density of mineral; that is, the black portions indicate the places where high density minerals exist such as zirconium and biotite. The preferential radial tensile cracks develop around the crushed zone, which occur along the current flow path. In addition, minor radial cracks, which have narrow crack width, are visible between the preferential cracks. The most radial cracks propagate with small fluctuations and branches with

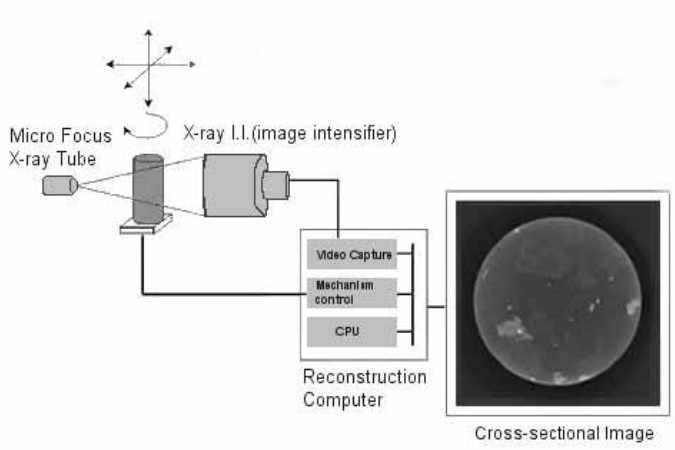

Fig.7 Schematic diagram of the microfocus X-ray CT system

great roughness near the surface. The crack branchings are due to the cracking from the surface. It is possible that the radial cracks from the current path speedily propagate regardless of rock constituents or minerals while the cracks near the surface generate at the boundaries of rock constituents. This means the existence of surface enhance the liberation of rock constituents and minerals. Spalling (tensile crack), which is generated by short shock pulse near the surface, is invisible. This implies that the mechanical stress caused by the high-voltage pulse in the solid dielectric has relatively longer pulse. It is noteworthy that two granite samples show two current paths. These multi-current paths are frequently caused when the rock sample include semi-conductive minerals such as zirconium. The number of fragments countered from CT images is compared with that observed by the naked eye in Table 2. This comparison shows that there exist more micro-cracks and minor cracks caused by the high-voltage-induced pulses and reflected waves from the surface.

In Fig. 8 (b), the radial tensile cracks around the current flow path and the cracks from the surface develop in the tuff samples. Almost cracks propagate along the boundaries of minerals.

In Fig. 8 (c), the radial tensile cracks develop linearly around the current flow path and some cracks have branchings near the surface. Shirahama sandstone is relatively homogenous material; therefore the radial crack could propagate with small roughness.

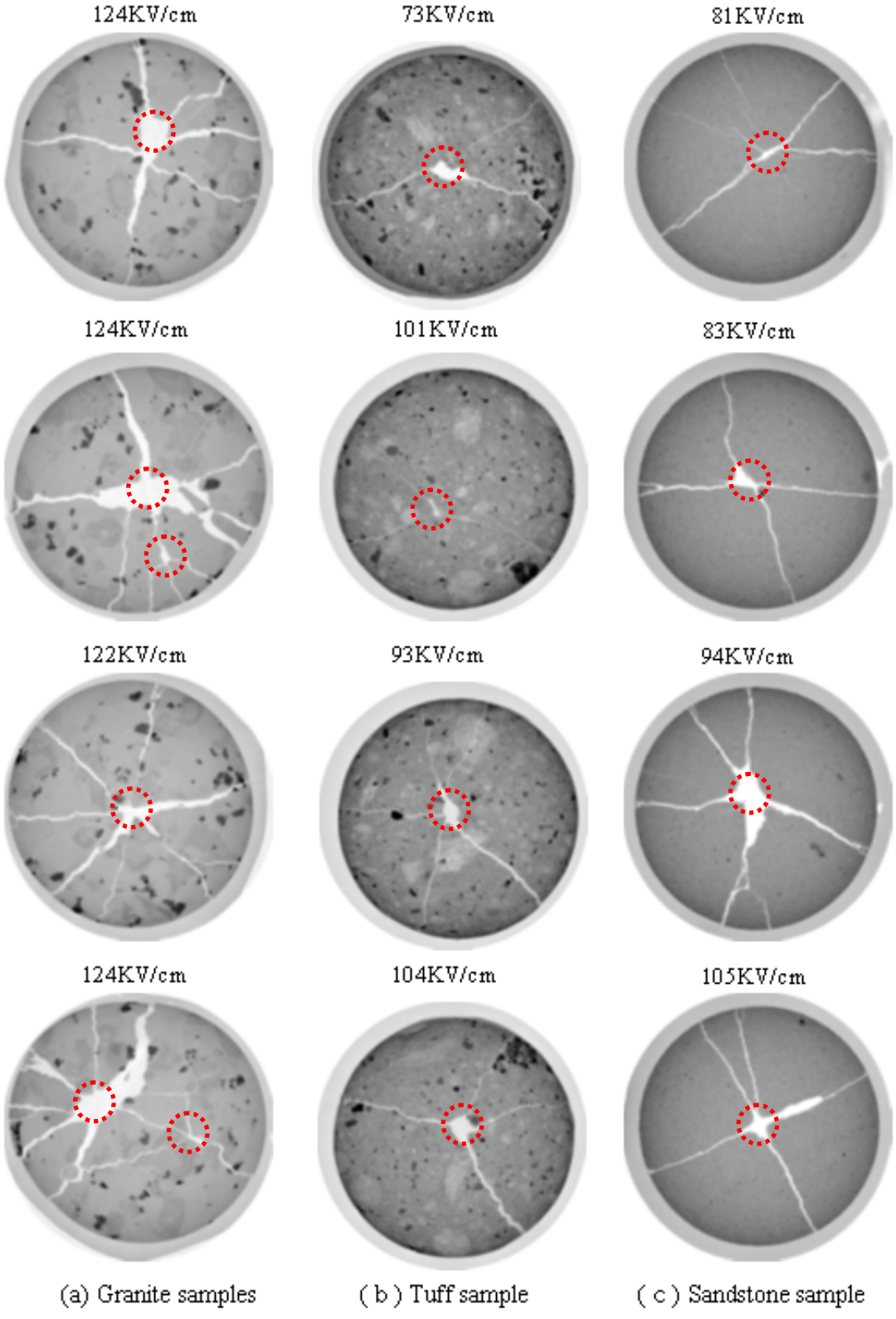

Fig. 8 Cross sectional image of X-Y slice for all tested samples; the dotted circle indicates the estimated current flow path.

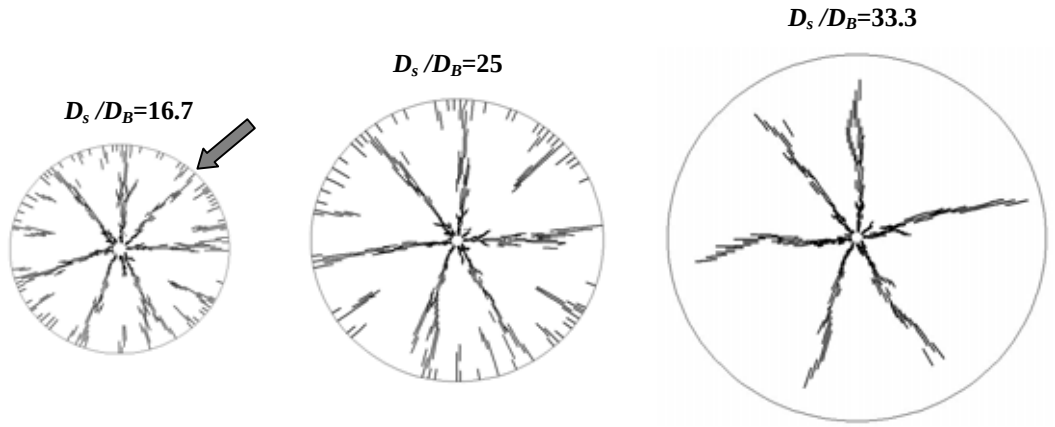

(a) D_s=10cm, T_0=100μs (b) D_s=15cm, T_0=100μs (c) D_s=20cm, T_0=100μs

Fig. 9 Fracture patterns of rock models with different sample sizes; Pressure loading rate P_0/T_0 reminds constant to 2MPa/μs.

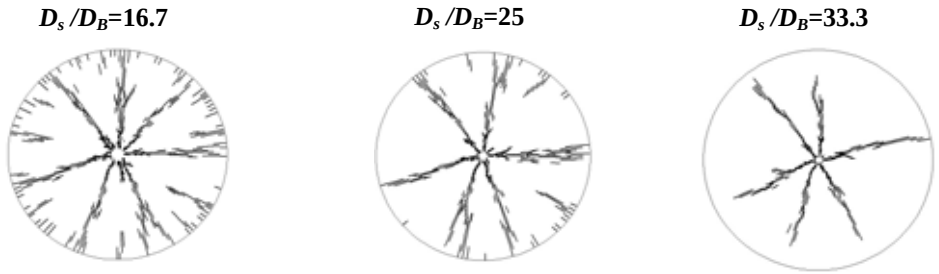

(a) D_b=6mm, T_0=100μs (b) D_b=4mm, T_0=100μs (c) D_b=3mm, T_0=100μs

Fig. 10 Fracture patterns of rock models with different bore-hole sizes; Pressure loading rate P_0/T_0 reminds constant to 2MPa/μs.

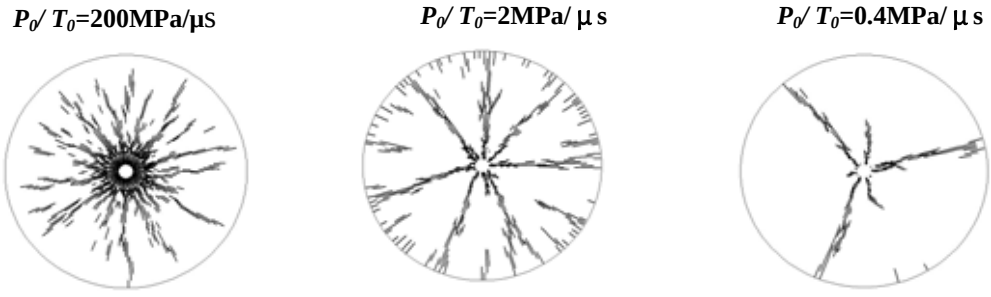

(a) D_s=10cm, T_0=1μs (b) D_s=10cm, T_0=100μs (c) D_s=10cm, T_0=500μs

Fig. 11 Fracture patterns of the rock models subjected to different pressure loading rates; D_s/D_B reminds constant to 16.7.

4. DISCUSSIONS OF THE DYNAMIC FRAGMENTATION OF ROCK

In section 2.2, Figure 4 showed that the number of fragments in the granite rock samples decreases with the diameter increase even though almost the same applied voltage and discharged current for all granite samples. This means that the resultant fracture patterns results from the size effect.

The dynamic fracture process analysis (DFPA) code [11] was used to simulate a stress-wave-induced fracture in the circular rock sample and investigate the effect of the sample size on the resultant fracture patterns. A circular model was used, consisting of a borehole in rock with a free surface. The diameter of the model D_s was changed as 10, 15 and 20 cm while the diameter of the borehole C_B remained constant as 6 mm. Elastic wave velocity was 5000 m/s and poison ratio was 0.25. The pressure waveforms with peak value of 200 MPa at time 100μs was applied to the wall of the borehole.

Figure 9 show the calculated resultant fracture patterns with different sample size. The fracture decreases with increasing size of the model. In Fig. 9(a), the radial cracks around the borehole propagated with small fluctuation and the cracks branched near the surface. The radial fracture plane indicated by the arrow was formatted by the crack generated from the surfaces. The fracture plane disappeared with increasing size of the model as shown in Fig. 9 (b). The crackings from the surface are invisible in Fig. 9(c).

The effect of the size of borehole on the fracture patterns was also investigated. Using the model in Fig. 9(a), the diameter of the borehole was changed as 4 and 3mm, considering the same D_s/D_B as the model of Figures 9 (a-c). Figure 10 show the resultant fracture patterns with different diameters of the borehole. It was confirmed that if loading condition and material properties are constant, the fracture patterns depend on the value of D_s/D_B.

The previous sections described that the number of fragments and fracture pattern varied with different rock types and applied voltages. According to Cho *et al.* [11], the fracture pattern is affected by the applied pressure loading rate. Using the model in Fig. 9(a), the rise time of pressure T_0 was changed as 1 and 500μs, considering the increasing applied pressure loading rate as 200, 2 and 0.4 MPa/μs.

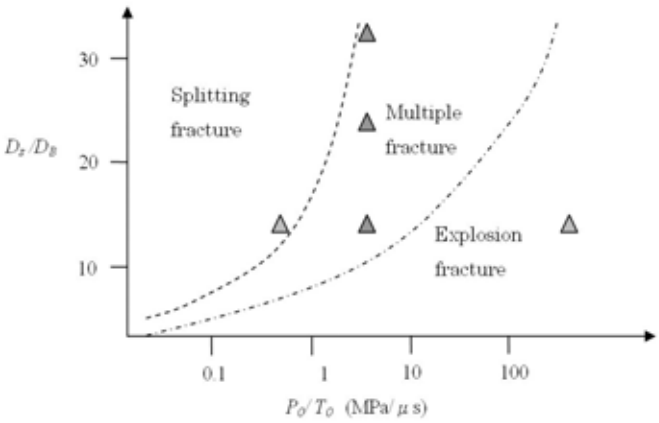

Fig. 12 Diagram representing the fracture pattern transition of circular rock model

Figure 11 show the resultant fracture patterns with different pressure loading rates. Cracks increased with the rise time. The increase in the number of cracks was associated with the stress-loading rates in the borehole.

As described above, the fracture pattern depends on the value of D_s/D_B and the applied pressure loading rate. In order to examine the transition condition between splitting fracture and explosion fracture in the circular rock model, the calculated fracture patterns in Fig. 9, 10 and 11 were analyzed and plotted in Fig. 12. The fracture transition could be divided as splitting fracture, multiple fracture and explosion fracture zone as shown in Fig. 12.

According to Bluhm *et al.* [8], in the electrical breakdown, the current flow channel creates a pressure of 1 to 10 GPa and is initially ~10 to 50 μm wide. With assuming that the current flow channel corresponds to the blast hole, D_s/D_b could be approximately 600. This may result in a fracture transition from multiple or explosion fractures zone to splitting or multiple fracture zone, even under the pressure of several GPa.

This study showed that the fracture pattern of rock by high-voltage pulses involves electric properties, material prosperities and geometry, and dynamic fracture processes of rock. Therefore, in order to control or improve the liberation efficiency of rock constituents using high-voltage pulses, the dynamic fragmentation of rock by high-voltage pulses has to be understood. It is possible that the study including the electric pulse dynamics and dynamic fracture process of rock will allow the optimization of the discharge parameters to improve the high-precise liberation of rock constituents.

5. CONCLUSION

Circular rock samples of three different types were fractured by high voltage pulses. The fragmentation process of rock by high-voltage pulses was summarized as follows.

a) Formation of the breakdown channel into the rock from the applied electrode with light emitting and propagation of the voltage discharge inside the rock; the voltage increases suddenly and reaches the peak value within 0.1 μs without increasing current.
b) Formation of the current flow channel between two electrodes; the voltage rapidly drops with increasing of the current.
c) Generation of mechanical stress caused by the expanding current flow channel; the current reaches the peak value within 1μs.
d) Crack propagation and crushing caused by the induced stress during several tens micro-second; while a bubble expands speedily over ten m/s.
e) Finally, disappearance of bubble after 3 ms and dispersion of fragments.

The fractures of the test samples were visualized and analyzed by using microfocus X-ray computed tomography (CT) system. In Inada granite samples, the preferential radial tensile cracks develop around the crushed zone, which occur along the current flow path. Minor radial cracks, which have narrow crack width, are visible between the preferential cracks. The most radial cracks propagated with small fluctuation and branched near the surface. In Tage tuff samples, the radial tensile cracks around the current flow path and the cracks from the surface develop. Almost cracks propagate along the boundaries of minerals. In Shirahama sandstone, the radial tensile cracks develop linearly around the current flow path and some cracks have branchings near the surface. The sandstone is relatively homogenous material; therefore the radial crack could propagate with small roughness.

The fracture patterns are simulated by using the dynamic fracture process analysis code and the fragmentation process resulting from electrical pulses are discussed.

6. ACKNOWLEDGEMENTS

Authors are thanks to Dr. Kodama, Horonobe Research Institute for Subsurface Environment, Japan. He kindly served Shirahama sandstone and Shikotsuko welded tuff.

REFERENCES

1. Budenstein, P.P, 1980, One mechanism of breakdown in solids, IEEE Trans, Electr. Insul. pp. 225-240
2. Andres, U, 1995, Electrical disintegration of rock, Mineral Processing and Extractive Metallurgy Review, Vol. 14, pp. 87-110
3. Owada, S., Ito, M., Ota, T., Nishimura, T., Ando, T., Yamashita, T. and Shinozaki, S., *Application of electrical disintegration to coal*, Proc. 22th Int. Miner. Process. Congr., 623-631 (2003a).
4. Ito, M., Owada, S, Cho, S.H., Nishimura, T., Nakagawa, Y., Yokota, M. and Kaneko, K., The effectives of mineralogica properties of samples on liberation phenomena in electrical disintergration, IMPC, Turkey, 2006 (in press)
5. Saini-Eidukat, B., Pedeson, B., and Weiblen, P.W., 1995, Use of electric pulse disaggregation to liberate fossils from North and South Dakota sediments, Proc., North Dakota Academy of Science, 87th Ann. Mtg., 20-21, Vol. 49, pp. 67
6. Touryan,K. J. Touryan,L. A. Benze, J. W., 1991, An Innovative Use of Pulsed Power Technology for Separation of Minerals from Ores, 8th IEEE International Pulsed Power Conference, San Diego, California (R. White and K. Prestwich, Editors), pp. 90-93
7. Fujita, T., Yoshimi, I., Tanaka, Y., Jeyadevan, B., and Miyazaki, T., *Research of Liberation by Using High Voltage Discharge Impulse and Electromagnetic Waves*, Shigen-to-Sozai (Journal of MMIJ), 115, 749-754 (1999).
8. Bluhm, H., Frey, W., Giese, H., Hoppe, P., Schultheib, C. and StrabnerR., 2000, Application of pulsed HV discharges to material fragmentation and recycling, IEEE Transaction on Dielectrics and Electrical Insulation, Vol. 7, No. 5, pp. 625-636
9. Inoue, H., Listitsyn, I., Akiyama, H. And Nishizawa, I, 2000, Drillings of hard rocks by pulsed power, IEEE Electronic Insulation Magazino, pp19-25
10. Cho, S.H., Ito, M., Yokota, M., Nakamiya, Y., Kubota, S., Ogata, Y., Owada, S., Mohanty, B. and Kaneko, K., 2006, Analysis of high-voltage pulse induced fractures by using micro X-ray CT system, (preparing)
11. Cho S.H. and Kaneko K., 2004, Influence of the applied pressure waveform on the dynamic fracture processes in rock, Int. J. Rock Mech. Min. Sci., Vol 41, 5, 771-784
12. Hammon, J., Hopwood, D., Ingram, M., Klatt, M. and Tatman, T., 2002, Electric pulse rock sample disaggregator, IEEE International Pulsed Power Conference, pp.1142-1145
13. Cho S.H., Yokota M., Ogata Y., Kobota S. and Kaneko K., 2005, Microscopic visualization in a granitic rock subjected to dynamic tensile loading by using microfocus X-ray CT, Science and Technology of Energetic Material Vol. 66, No.4 pp. 3348-339